HEFAT2012
9th International Conference on Heat Transfer, Fluid Mechanics and Thermodynamics
16 – 18 July 2012
Malta

SINGLE-PHASE CONVECTIVE HEAT TRANSFER AND PRESSURE DROP COEFFICIENTS IN SMOOTH CONCENTRIC ANNULI

Van Zyl W.R., Dirker J.,*, Meyer J.P.
*Author for correspondence
Department of Mechanical and Aeronautical Engineering,
University of Pretoria,
Pretoria, 0002,
South Africa,
E-mail: jaco.dirker@up.ac.za

ABSTRACT

Varying diameter ratios associated with smooth concentric tube-in-tube heat exchangers are known to have an effect on its convective heat transfer capabilities. Linear and nonlinear regression models exist for determining the heat transfer coefficients; however these are complex and time consuming, and require much experimental data in order to obtain accurate solutions. A large dataset of experimental measurements on heat exchangers with annular diameter ratios of 0.483, 0.579, 0.593 and 0.712 was gathered. Using the modified Wilson plot technique, a nonlinear regression scheme, and the log mean temperature difference method, both local and average Nusselt numbers were determined. Local wall temperature measurements were made using a novel method. Friction factors were calculated directly from measured pressure drops across the annulus. Both heated and cooled horizontal annuli with Reynolds numbers based on the hydraulic diameter varying from 10 000 to 45 000 with water as the working medium were investigated.

INTRODUCTION

Convection heat transfer is the main heat transfer mechanism in most heat exchangers. It is thus essential that the convection heat transfer and friction factors are thoroughly understood in order to optimally design heat exchangers. The tube-in-tube heat exchanger with a counter flow configuration operating in the turbulent flow regime is one of the simplest types of heat exchangers. Correlations for the heat transfer coefficients and friction factors for such heat exchanger types have been found to be inconsistent with each other. The annular diameter ratio, which is defined as the ratio of the inner tube's outer diameter to the outer tube's inner diameter have been reported to influence both the heat transfer and pressure drop within the annulus. Due to the complexities of turbulent flow it is required that experimental data is used to determine correlations for heat transfer coefficients and friction factors within the annulus.

NOMENCLATURE

a	[-]	Annular diameter ratio
A_s	[m^2]	Surface area
A_o	[m^2]	Cross sectional area of annulus
C_i	[-]	Inner tube correlation coefficient
C_o	[-]	Outer tube correlation coefficient
Cp	[J/kgK]	Specific heat
CV	[-]	Control volume
D_h	[m]	Hydraulic diameter
eb	[%]	Energy Balance
f	[-]	Friction factor
F_{ann}	[-]	Factor taking into account the dependence on a
h	[W/m^{2}K]	Convective heat transfer coefficient
j	[-]	Index number
k	[W/mK]	Thermal conductivity
K	[-]	Factor to take into account the temperature dependence of fluid properties
L_{dp}	[m]	Pressure drop length
L_{hx}	[m]	Heat exchange length
$\dot{m}$	[kg/s]	Mass flow rate
N_i	[-]	Number of thermocouples on inner tube
Nu	[-]	Nusselt number
n	[-]	Exponent
P	[-]	Reynolds number exponent
Pr	[-]	Prandtl number
Δp	[Pa]	Pressure drop
$\dot{Q}$	[W]	Heat transfer rate
$\bar{Q}$	[W]	Average heat transfer rate
Re	[-]	Reynolds number
Re^*	[-]	Modified Reynolds number, Equation (2) and (15)
T	[°C]	Temperature
ΔT_{LMTD}	[°C]	Logarithmic mean temperature difference
$\bar{T}$	[°C]	Average temperature
V	[m/s]	Fluid velocity
x	[m]	Axial length along the heat exchanger

Special characters

μ	[m^2/s]	Kinematic viscosity
ρ	[kg/m^3]	Density
φ	[-]	Factor in Equation (2)

Subscripts

1	Inner tube outer wall
b	Bulk property
Dh	Based on hydraulic diameter
i	Inner tube

ii	Inner tube inlet
io	Inner tube outlet
local	Local property
o	Annulus
oi	Annulus inlet
oo	Annulus outlet
w	Wall

Table 1 provides recently published correlations for determining Nusselt numbers. Gnielinski [1] based a correlation on heat transfer coefficients in turbulent pipe flow, and was extended to include effects of the annular diameter ratio. Dirker and Meyer [2] investigated eleven available correlations and compared them to data obtained from their work. They found differences of up to 20% in the available correlations and as a result, presented their own correlation. Gnielinski [3] modified the correlation in [1] to fit more recent experimental data including that of Dirker and Meyer [2] Gnielinski [3] also reports that the heat transfer is influenced by the direction of heat flux across the wall when the fluids physical properties are temperature dependent (no direct investigations into the effect of the direction of heat flux across the wall are known). Lu and Wang [4] investigated heat transfer characteristics of water flow through both a horizontal and vertical annulus with an annular diameter ratio of 0.795. Swamee et al [5] modified the smooth tube Sieder and Tate correlation to optimize the design of tube-in-tube heat exchangers.

The friction factor within an annulus is also dependent on annular ratio, and differ from that of a circular tube due to the different velocity profiles in annular flow. Table 2 provides available correlations for friction factors within an annulus. Kaneda et al [6] performed direct numerical simulations on annular flow and proposed their equation based on wall shear stresses. Jones and Leung [7] used a laminar correction factor for smooth annuli to modify the Reynolds number based on hydraulic diameter. This modification was used in the Prandtl friction factor for turbulent flow in smooth tubes. Gnielinski [3] used a large number of available experimental data to produce a correlation which was based on a modified correlation for turbulent friction factors in smooth tubes. As with the heat transfer correlations, there are no known investigations regarding the influence of the direction of heat flux.

In this study large data sets with relatively high accuracy were gathered. Both heated and cooled annuli were tested to consider the effects of the direction of heat flux across the wall on both heat transfer coefficients and friction factors. Wall temperatures on both the inner tube wall and annulus wall were measured directly. Using the wall temperature measurements local heat transfer coefficients in the annulus were investigated.

Table 1: Existing Nusselt number correlations for annular passages.

Author(s)	Correlation	Eq	Diameter Ratio Range (a)	Reynolds number range (Re_{Dh})	Working fluid
Dirker and Meyer [2]	$Nu_{Dh} = C_o Re_{D_h}^{P} Pr^{1/3} \left(\frac{\mu_o}{\mu_{iw}}\right)^{0.14}$ $P = 1.013e^{-0.067/a}$ $C_o = \frac{0.003a^{1.86}}{0.063a^{-3} - 0.0674a^{-2} + 2.225/a - 1.157}$	(1)	0.3125 – 0.588	4000 – 30 000	Water
Gnielinski [3]	$Nu_{Dh} = \frac{\left(f/8\right) Re_{Dh} Pr_o}{\varphi + 12.7\sqrt{f/8}\left(Pr_o^{2/3} - 1\right)}\left[1 + \left(\frac{D_h}{L_{hx}}\right)^{2/3}\right] F_{ann} K$ $\varphi = 1.07 + \frac{900}{Re_{Dh}} - \frac{0.63}{(1 + 10Pr_o)}$ $K = \left(\frac{Pr_o}{Pr_{iw}}\right)^{0.11}$ for liquids $K = \left(\frac{T_b}{T_{iw}}\right)^{n}$ for gases with $n = 0$ for cooling $n = 0.45$ for $0.5 < \frac{T_b}{T_{iw}} < 1.0$ $F_{ann} = 0.75a^{-0.17}$ $f = (1.8\log_{10} Re^{*} - 1.5)^{-2}$ $Re^{*} = Re_{Dh}\frac{(1 + a^2)\ln a + (1 - a^2)}{(1 - a)^2 \ln a}$	(2)	Not Specified	Not Specified	All media
Lu and Wang [4]	$Nu_{Dh} = 0.0022 Re_{Dh}^{1.09} Pr_o^{0.4}$	(3)	0.6911	> 3 000	Water
Swamee et al [5]	$Nu_{Dh} = \frac{0.027}{(1 + 1/a)^{0.2}} Re_{Dh}^{0.8} Pr_o^{1/3} \left(\frac{\mu_o}{\mu_{iw}}\right)^{0.14}$	(4)	Not specified	Not Specified	Not specified
Dittus and Boelter [8]	$Nu_{Dh} = 0.023 Re_{D_h}^{0.8} Pr_o^{n}$ $n = 0.4$ for heating $n = 0.3$ for cooling	(5)	Not specified	> 10 000	Not specified

DEFINITIONS

Figure 1 shows a cross sectional view of the heat exchanger indicating relevant dimensions and boundary conditions. Heat is transferred at the inner wall with the outer wall insulated. The mean annulus heat transfer coefficient is defined as:

$$h = \frac{\bar{Q}}{A_s \Delta T_{LMTD}} \tag{6}$$

With A_s the wall surface area and $\bar{Q}$ the average rate of heat transfer to the fluid given as:

$$\bar{Q} = \frac{\dot{Q}_i + \dot{Q}_o}{2} \tag{7}$$

The logarithmic mean temperature difference for the annulus side (ΔT_{LMTD}) is defined as:

$$\Delta T_{LMTD} = \frac{(\bar{T}_{iw} - T_{oi}) - (\bar{T}_{iw} - T_{oo})}{\ln[(\bar{T}_{iw} - T_{oo})/(\bar{T}_{iw} - T_{oi})]} \tag{8}$$

With $\bar{T}_{iw}$ the mean wall temperature, T_{oi} the annulus inlet temperature and T_{oo} the annulus outlet temperature of the fluid. The dimensionless Nusselt number is defined as:

$$Nu_{Dh} = \frac{hD_h}{k} \tag{9}$$

Where D_h is the hydraulic diameter defined as:

$$D_h = D_o - D_1 \tag{10}$$

The friction factor of the duct is defined as:

$$f = \frac{2D_h \Delta p}{\rho L_{dp} V^2} \tag{11}$$

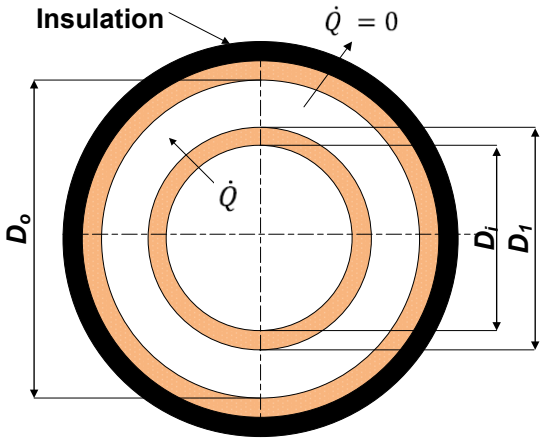

Figure 1: Cross section and boundary conditions of tube-in-tube heat exchanger.

Where Δp is the pressure drop of the fluid along length L_{dp} of the annulus. Both heat transfer coefficients and friction factors are dependent on the annular diameter ratio defined as

$$a = \frac{D_1}{D_o} \qquad (0 \le a \le 1) \tag{12}$$

Here the limiting case of a = 0, is a circular tube with an infinitesimal thin wire at the centre and a = 1, is parallel plate geometry.

Fluid properties were calculated from formulae proposed by Popiel and Wojtkowiak [9] at the average bulk temperature approximated as:

$$T_b = \frac{T_{oi} + T_{oo}}{2} \tag{13}$$

Table 2: Existing friction factor correlations for annular ducts.

Author(s)	Correlation	Eq	Diameter Ratio Range(a)	Reynolds Number Range (Re_{Dh})	Working Fluid
Kaneda et al [6]	$\frac{f}{8} = \left[1.61 + \frac{1}{0.436}\ln\left(\frac{Re_{Dh}}{\sqrt{8/f}}\right) - \frac{550}{Re_{Dh}\sqrt{f/8}}\right]^{-2}$	(14)	0.0 – 1.0	> 10 000	Not specified
Jones and Leung [7]	$\frac{1}{\sqrt{f}} = 2\log_{10} Re^*\sqrt{f} - 0.8$ $Re^* = Re_{Dh}\frac{(1+a^2)\ln a + (1-a^2)}{(1-a)^2 \ln a}$	(15)	0.0 – 1.0	10 000 – 1,000,000	Based on other authors data.
Gnielinski [3]	$\frac{1}{\sqrt{f}} = 1.8\log_{10} Re^* - 1.5$ $Re^* = Re_{Dh}\frac{(1+a^2)\ln a + (1-a^2)}{(1-a)^2 \ln a}$	(16)	Not specified	Not specified	All Media
Blasius [10]	$f = 0.3164 Re_{Dh}^{-0.25}$	(17)	Not specified	Not specified	All Media

The Reynolds number based on the hydraulic diameter of the annulus is defined as:

$$Re_{Dh} = \frac{\dot{m}_o D_h}{\mu_o A_o} \tag{18}$$

The heat transfer rate of the fluid was calculated as:

$$\dot{Q} = \dot{m} Cp (T_{oi} - T_{oo}) \tag{19}$$

EXPERIMENTAL FACILITY

The experimental facility was a closed loop system designed in such a way as to accommodate heat exchangers of different sizes, with the option of having either a heated or cooled annulus. Refer to Figure 2. Block **i** represents the cold water supply and block **ii** the warm water supply. In the current configuration a cooled annulus is represented.

Cold water was stored in a 1 000 ℓ tank (item 2) and connected to a 16 kW cooling unit (item 1). Valves (items 4a and 4b) were used to control fluid flow, to either the test section or returned to the storage tank in a bypass line. Water in the inner tube was pumped using a positive displacement pump (item 3a) with a maximum flow rate of 1 900 ℓ/h. The flow rate was controlled using a vector drive coupled to the pump motor. Pulsations in the flow were damped using a 4 ℓ accumulator (item 5a). Fluid flow rates were obtained with a Coriolis flow meter (item 6a) with an effective range of 54.5 ℓ/h – 2 180 ℓ/h. The water passed through the inner tube of the test section (item 10) and returned to the storage tank. A non-return valve (item 7a) was used to avoid back flow.

The annulus loop was equipped with a 600 ℓ storage tank (item 8) and heated with a 12 kW electrical resistance heater. The water in the annulus was pumped using a 6 000 ℓ/h centrifugal pump. Valves (items 4c and 4d) were used to control fluid flow, to either the test section or returned to the storage tank in a bypass line. The flow rate was controlled using a vector drive coupled to the pump motor. Pulsations in the flow were damped using a 10 ℓ accumulator (item 5b). A Coriolis flow metre (item 6b) with a range from 170 ℓ/h – 6 800 ℓ/h was fitted to measure flow rates. The water passed through the test section (item 10). A non-return valve (item 7b) was used to prevent back flow.

Three pressure transducers with interchangeable diaphragms (item 9) were connected to the inlet and outlet of the annulus. The three pressure transducers are calibrated from 0 kPa - 22 kPa, 0 kPa - 35 kPa and 0 kPa - 140 kPa with accuracies of 0.25% of their full scale values. Each diaphragm used with the differential pressure transducer was calibrated using a dead weight system.

All thermocouples were calibrated against a Pt100 with a manufacturer specified uncertainty of 0.1°C. Using the method of Kline and McClintock [11] uncertainties on the instruments were determined and are shown in Table 3.

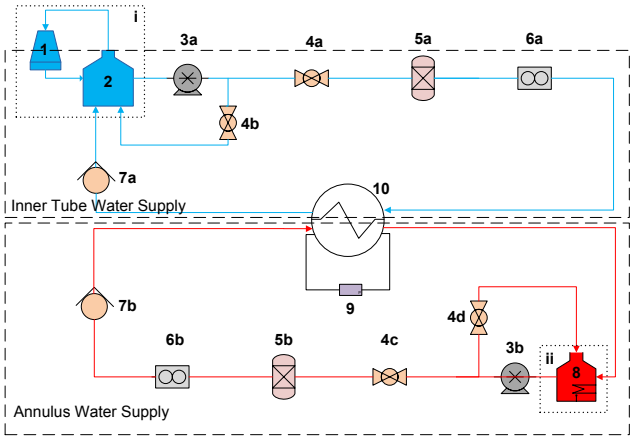

Figure 2: Experimental test facility.

Table 3: Uncertainties of instrumentation.

Item	Instrument	Range	Uncertainty
	Thermocouple	-200 - 350°C	± 0.1°C
6(a)	Flow meter	0.015 - 0.603 kg/s	± 0.1%^{r}
6(b)	Flow meter	0.047 - 1.883 kg/s	± 0.1%^{r}
9	Differential pressure transducers	0-21 kPa	± 2.0%^{fs}
		0-35 kPa	± 2.2%^{fs}
		0-140 kPa	± 2.6%^{fs}

fs: Percentage of full scale value.
r: Percentage of reading.

The resulting uncertainties of the mean Nusselt number, averaged local Nusselt number and friction factors are ± 1.8%, ± 2.6% and ± 0.8% respectively.

TEST SECTION

A total of four counter flow heat exchanger test sections shown in Figure 3 were built and tested. Major dimensions are included in Table 4. The inner tube was constructed from a 5.5m long hard drawn copper tube. Nine measurement stations were equally spaced along the length of the inner tube. Each station had two T-type thermocouples attached and spaced 180° apart within the inner tube wall.

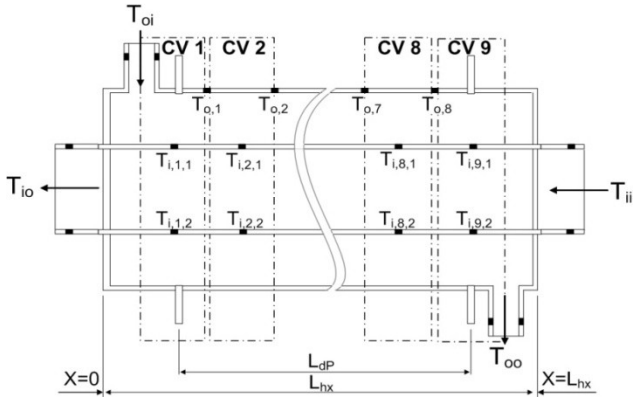

Figure 3: Heat exchanger separated into nine control volumes.

Table 4: Dimensions of test sections (refer to Figure 1 and Figure 3).

Heat Exch-anger	D_i (mm)	D_1 (mm)	D_o (mm)	a (-)	L_{hx} (m)	L_{dp} (m)
1	14.46	15.88	32.89	0.483	4.85	4.79
2	17.63	19.05	32.89	0.579	5.30	4.98
3	14.46	15.88	26.76	0.593	4.85	4.79
4	17.63	19.05	26.76	0.712	5.06	5.00

Figure 4 shows the attachment of the thermocouples within a section of the inner tube wall. This was achieved by machining a groove into the tube wall and soldering the thermocouple junctions within the groove, leaving no protrusions on the inner tube outer wall. The thermocouples were fed through a 1.2mm diameter hole drilled through the inner tube wall and retrieved at the ends of the inner tube. The tube was parted near the centre to simplify feeding the thermocouples through the tube. The tube was later reattached with a copper bush on the inner tube inner wall as a support ensuring concentricity. Four thermocouples were attached and spaced at 90° intervals around the periphery of the inner tube inlet and outlet.

The outer tube was constructed from eight hard drawn copper sections 625 mm in length. They were attached concentrically around the inner tube using spacers integrated into straight couplings. Figure 5 shows a cross section of the couplings used. On each section a thermocouple was placed on the outer wall of the annulus tube. Sufficient insulation was placed around the annulus tube.

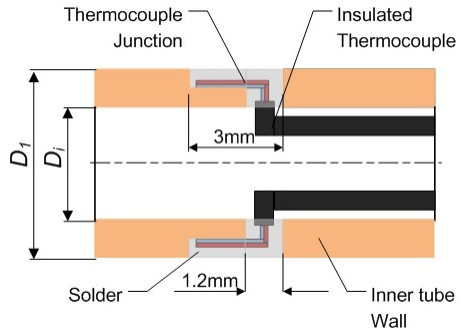

Figure 4: Attachment of thermocouples to inner tube wall.

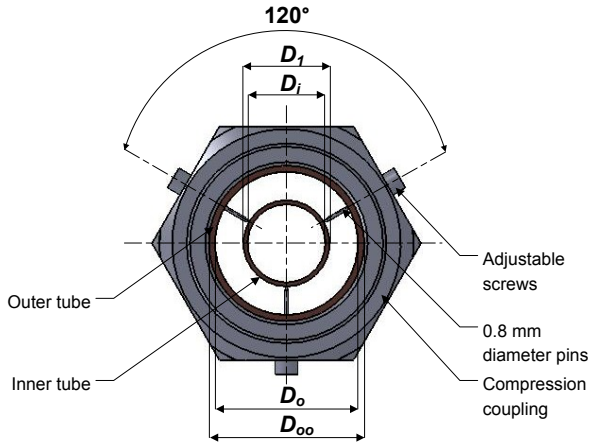

Figure 5: Spacers integrated into couplings.

Pressure drops across the annulus length are measured by means of pressure taps fixed on the outer walls of the annulus. Two pressure taps 180° apart were located at the inlet and two at the outlet of the annulus.

EXPERIMENTAL PROCEDURE

Experimental tests were performed over a wide range of flow rate combinations of the inner tube and annulus. A larger spectrum of annular flow rates was covered, due to the annulus being of primary interest in this study. Experiments were performed with the inlet temperatures to the annulus and inner tube constant. The inner tube flow rate was held constant while altering the annular flow rate through a spectrum. Once sufficient data points were captured, the inner tube flow rate was altered and the process repeated. Data was logged once steady state conditions were reached and desirable energy balances were obtained. Acceptable steady state conditions were when the inner tube and annulus outlet temperatures changed by less than 0.1°C over 30 seconds. This procedure was performed for the case of both a heated annulus and cooled annulus. Energy balances below 2% and 4% for a heated and cooled annulus respectively, were achieved, where the energy balance is calculated as:

$$eb = \frac{|\dot{Q}_i - \dot{Q}_o|}{(\dot{Q}_i + \dot{Q}_o)/2} \tag{20}$$

DATA REDUCTION

Three methods were used to calculate the heat transfer coefficients, namely the modified Wilson plot method of Briggs and Young [12], the non-linear regression scheme of Khartabil and Christensen [13] and the logarithmic mean temperature difference (LMTD) method.

Method 1: Linear Regression Scheme

Using a linear regression analysis, the modified Wilson Plot method of Briggs and Young [12] solves the three constants C_i, C_o and P of the Sieder and Tate type equations.

$$Nu_i = \frac{h_i D_i}{k_i} = C_i Re_i^{0.8} Pr_i^{\frac{1}{3}} \left(\frac{\mu_i}{\mu_{iw,i}}\right)^{0.14} \tag{21}$$

$$Nu_{Dh} = \frac{h_o D_h}{k_o} = C_o Re_{D_h}^{P} Pr_o^{\frac{1}{3}} \left(\frac{\mu_o}{\mu_{iw,o}}\right)^{0.14} \tag{22}$$

Where $\mu_{iw,i}$ and $\mu_{iw,o}$ are the fluid viscosities at the inner surface and outer surface of the inner wall respectively. This method requires a large data set of inlet and outlet temperatures as well as fluid flow rates for both the inner tube and annulus.

Method 2: Non-Linear Regression Scheme

The method of Khartabil and Christensen [13] uses a non-linear regression model to determine the coefficients C_i, C_o and P of the Sieder and Tate type equation given in Equations (21) and (22). By determining the values of C_i and C_o through Gauss

elimination, P is solved numerically using a numerical bisection method.

Method 3: LMTD Method

The LMTD method is used to calculate both the mean heat transfer coefficients as well as the local heat transfer coefficients. To determine the mean heat transfer coefficients, the inner wall temperature is taken as the average of the measured wall temperatures of the inner wall:

$$\bar{T}_{iw} = \frac{1}{N_i}\sum_{j=1}^{N_i} T_{iw,j} \tag{23}$$

Where $\bar{T}_{iw}$ is the average inner wall temperature and N_i the number of thermocouples placed on the inner wall (eighteen were used in this study). The ΔT_{LMTD} is then calculated with Equation (8). The mean heat transfer rate is calculated with Equation (7). The annulus heat transfer coefficient is then determined from Equation (6).

To calculate the local heat transfer coefficients, the heat exchanger was divided equally into nine control volumes along length L_{hx}, and arranged as in Figure 3. Here the thermocouples on the outer tube wall measure the annulus fluid temperature.

The local ΔT_{LMTD} is calculated as

$$\Delta T_{LMTD,CV,j} = \frac{T_{oi,CV,j} - T_{oo,CV,j}}{\ln\left[\left(T_{iw,CV,j} - T_{oo,CV,j}\right)/\left(T_{iw,CV,j} - T_{oi,CV,j}\right)\right]} \tag{24}$$

Here the subscript CV refers to the associated local property of control volume j, where j = 1...9. The outer inlet and outer outlet temperatures are obtained from temperatures measured on the outer tube wall, therefore:

$$T_{oi,CV,j} = T_{o,j-1} \tag{25}$$

$$T_{oo,CV,j} = T_{o,j} \tag{26}$$

Control volumes one and nine located at the annulus inlet and outlet will have:

$$T_{oi,CV,1} = T_{oi} \tag{27}$$

$$T_{oo,CV,9} = T_{oo} \tag{28}$$

The inner wall temperature is then:

$$T_{iw,CV,j} = \frac{\left(T_{i,j,1} + T_{i,j,2}\right)}{2} \tag{29}$$

Local fluid properties are calculated at the control volume bulk temperature:

$$T_{b,CV} = \frac{T_{oi,CV,j} + T_{oo,CV,j}}{2} \tag{30}$$

The annulus rate of heat transfer for each of the control volumes is:

$$\dot{Q}_{o,CV,j} = \dot{m}_{o,CV,j} Cp_{o,CV,j}\left(T_{oo,CV,j} - T_{oi,CV,j}\right) \tag{31}$$

The annulus local heat transfer coefficient is:

$$h_{o,LMTD,CV,j} = \frac{\dot{Q}_{o,CV,j}}{A_{s,CV,j}\Delta T_{LMTD,CV,j}} \tag{32}$$

Local Reynolds numbers are calculated for each control volume with

$$Re_{o,CV,j} = \frac{\dot{m}_{o,CV,j} D_h}{\mu_{o,CV,j} A_o} \tag{33}$$

Where $\dot{m}_{o,CV,j}$ are equal for all control volumes, and $\mu_{o,CV,j}$ is calculated at $T_{b,CV}$.

RESULTS

The four annular diameter ratios that were tested showed that both the heat transfer coefficients and friction factors depend on the direction of heat flux at the inner wall, as well as the annular diameter ratio.

Mean Nusselt Number

Mean experimental Nusselt numbers determined using the linear and nonlinear regression schemes, and the LMTD method for the heat exchanger with a = 0.593 are shown in Figure 6 and Figure 7 for a heated and cooled annulus respectively. The correlations in Table 1 are also shown in Figure 6 and Figure 7, for a cooled and heated annulus respectively.

For a cooled annulus the correlations in Table 1 seem to under predicted the results of the linear and nonlinear regression schemes. The correlations of Dirker and Meyer [2], Gnielinski [3] and Dittus and Boelter [8] corrlelated with the LMTD results within 3%.

For a heated annulus all existing correlations in Table 1 showed an under prediction of the Nusselt numbers. The differences for the linear and non linear regression schemes were up to 20% when compared to the correlations of Dirker and Meyer [2].

Noticeable differences in Nusselt numbers were observed depending on the direction of heat flux. A heated annulus resulted in a 20% larger Nusselt number than for a cooled annulus. Similar tests performed in Ntuli *et al* [14] also showed Nusselt numbers for a heated annulus were 20% larger than those of a cooled annulus. This is due to the higher viscosity of the of the cooler annulus fluid for the heated annulus. Figure 8 and Figure 9, for a cooled and heated annulus respectively, show the effect of altering the annular diameter ratio on the Nusselt number for a specific annulus and inner tube Reynolds number.

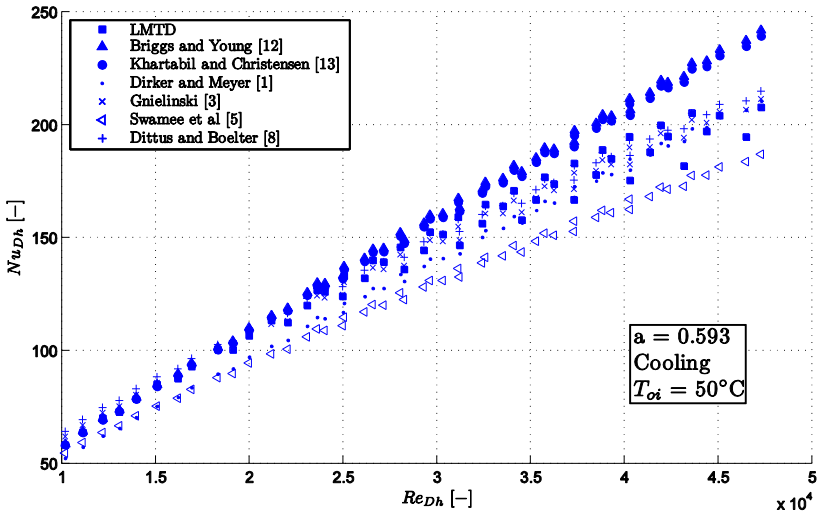

Figure 6: Mean Nusselt numbers for a cooled annulus.

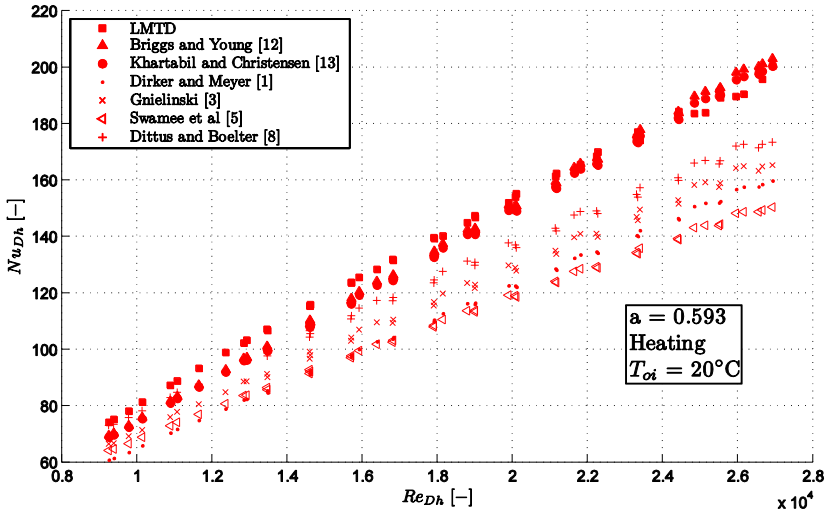

Figure 7: Mean Nusselt numbers for a heated annulus.

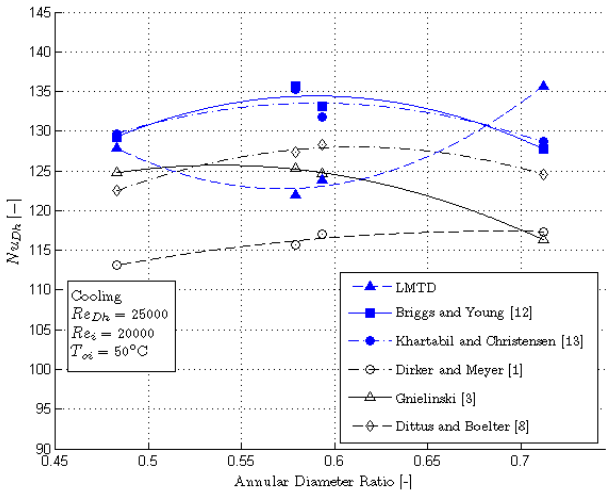

Figure 8: Nusselt numbers for a cooled annulus and four annular diameter ratios.

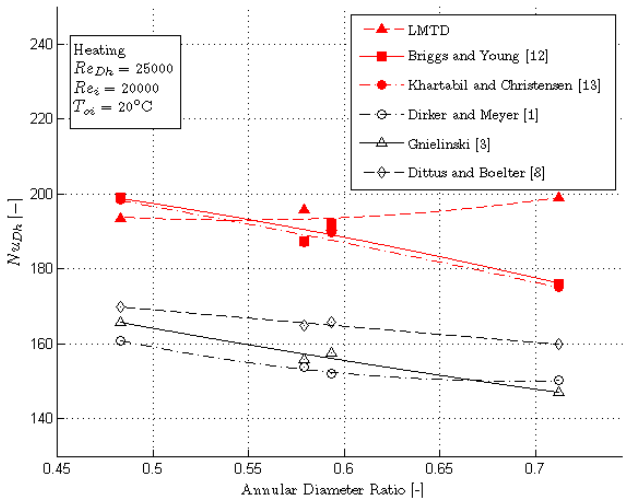

Figure 9: Nusselt numbers for a heated annulus, and four annular diameter ratios.

The methods of Briggs and Young [12], Khartabil and Christensen [13] and the *LMTD* are compared to existing correlations. Figure 8 and Figure 9 were plotted at various other Reynolds number combinations and similar trends were observed. The linear and nonlinear regression analysis produce results within 0.5% of each other, however there is no similarity to the *LMTD* method.

Local Nusselt Numbers

The local heat transfer is highly sensitive to wall temperature errors on both the inner tube wall and outer tube wall. A sensitivity analysis showed that an error of 1°C on the inner tube wall resulted in a local Nusselt number error in excess of 160%. Both the inner tube and outer tube wall showed a linear temperature profile along the axial length of the heat exchanger, shown in Figure 10. All combinations of inner and annular Reynolds numbers showed similar trends. Eliminating measurement errors using a linear fit of the wall temperature data, the local Nusselt numbers along the axial length of the heat exchanger were calculated. Figure 11 and Figure 12 show the local Nusselt numbers along the heat exchanger length for specific local Reynolds numbers for a cooled and heated annulus respectively.

Figure 11 and Figure 12 were plotted at various other inner tube annular Reynolds number combinations and similar trends were observed for all combinations. The decrease from annulus inlet to annulus outlet is dependent on the local Reynolds number, as larger decreases are observed with larger local Reynolds numbers. The largest Nusselt numbers occur at the inlet of the annulus and decreases towards the annulus outlet. The average local Nusselt number calculated over the heat exchanger length is given as:

$$\overline{Nu}_{Dh,Local} = \frac{1}{N_{CV}-1}\sum_{j=2}^{N_{CV}-1} Nu_{CV,j} \tag{34}$$

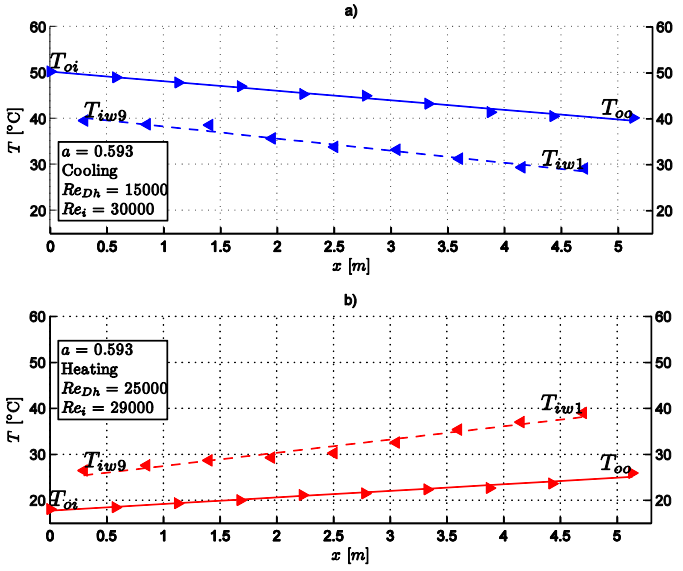

Figure 10: Inner and outer wall temperature profiles for a) cooled annulus and b) heated annulus.

The average local Nusselt numbers fall within 7% of the mean Nusselt number and within 3% of the Dirker and Meyer [2] correlation for a cooled annulus. For a heated annulus the average local Nusselt numbers fall within 14% of the mean Nusselt number and 1.5% of the Dirker and Meyer [2] correlation. This agreement can be attributed to the length of test set ups that were used by Dirker and Meyer [2] which were similar to those used here. It can be seen from Figure 11and Figure 12 that the length of a heat exchanger will have a significant impact on the average Nusselt numbers, depending on the distance of the local points from the inlet. Different researcher used different test section lengths; this may explain the disagreement in the results.

Friction Factor

Figure 13 and Figure 14, for a cooled and heated annulus respectively, show the effects of altering the annular diameter ratio on friction factors for a specific Reynolds number. Both a cooled and heated annulus shows that for $a < 0.64$ the correlations of Table 2 under predict the friction factors. However for $a > 0.62$ the correlations of Jones and Leung [7] and Gnielinski [3] over predict the friction factors while the correlations of Kaneda et al [6] and Blasius under predict the friction factors. A cooled annulus showed friction factors up to 9% larger than the friction factors of a heated annulus.

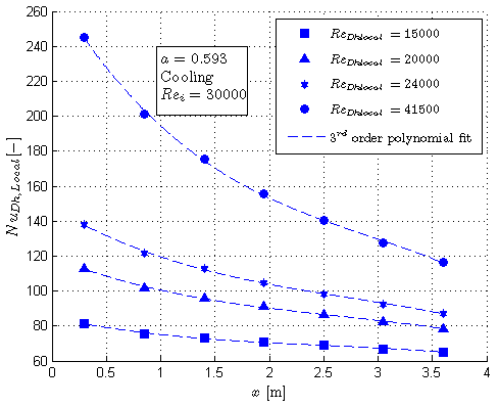

Figure 11: Nusselt numbers for various local Reynolds numbers for a cooled annulus.

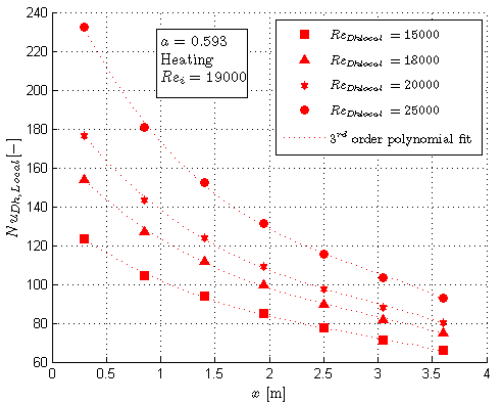

Figure 12: Nusselt numbers for various local Reynolds numbers for a heated annulus.

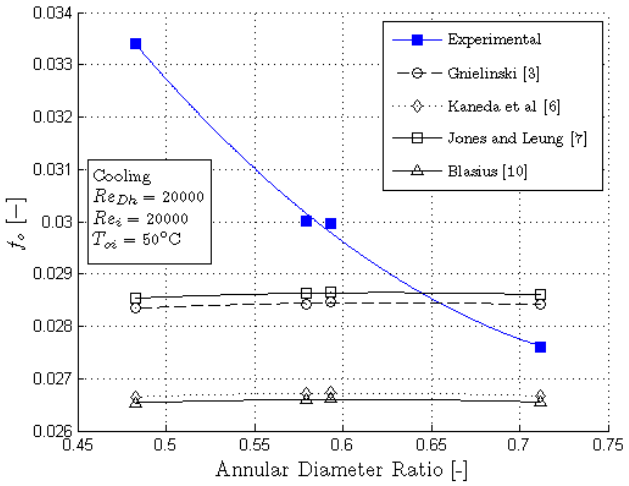

Figure 13: Friction factors for a cooled annulus.

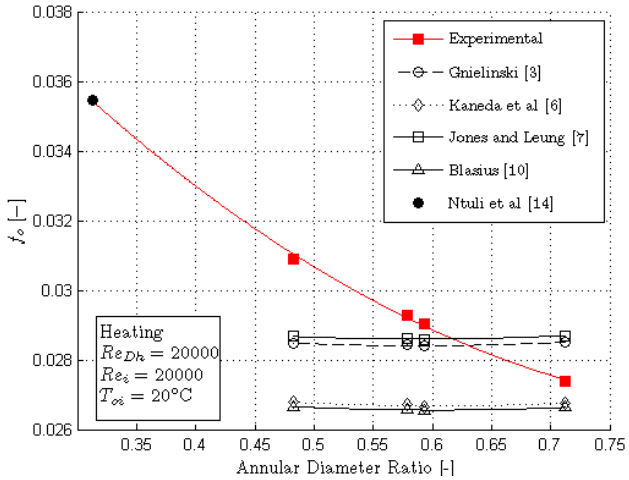

Figure 14: Friction factors for a heated annulus.

Ntuli et al [14] performed similar tests as reported on here for an annular diameter ratio of 0.313. The friction factor for a heated annulus from their results is included on Figure 14.

CONCLUSION

Four heat exchangers were tested for two different heat flux directions across the wall, namely a heated and cooled annulus. The direction of heat flux across the wall affected both the annulus heat transfer and friction factors. A heated annulus showed Nusselt numbers that were on average 20% larger than a cooled annulus. This results from the wall temperatures of the heated annulus being lower than those of a cooled annulus. Friction factors for a heated annulus were on average 9% lower than a cooled annulus.

Altering the annular diameter ratio affected both the annulus Nusselt numbers and friction factors. The effects of altering the annular diameter ratio on the Nusselt numbers were inconclusive as there was a disagreement between the three analysis methods used.

The annular diameter ratio has a greater influence on the friction factor than any of the existing correlations predict. The friction factors decrease with an increasing annular diameter ratio by 10% for the range annular diameter ratios investigated. Local Nusselt numbers along the axial length of the heat exchanger showed a maximum local Nusselt number occurring at the annulus inlet, and decreasing towards the annulus outlet.

RECOMMENDATIONS

To minimize uncertainties on the inner wall temperature measurements, additional thermocouples could be used around the periphery of the inner tube. Due to larger energy balance errors for a cooled annulus, more effective methods of providing insulation could be used. Additional data could be collected for a wider range of annular diameter ratios to further investigate the effects of the local Nusselt numbers along the axial length of the test section.

REFERENCES

[1] V Gnielinski, "VDI-Heat Atlas," *VDI-Verlag, Section GD*, 1993.

[2] J Dirker and J.P Meyer, "Convection Heat Transfer in Concentric Annuli," *Experimental Heat and Mass Transfer*, vol. 17, pp. 19-29, 2004.

[3] V Gnielinski, "Heat Transfer Coefficients for Turbulent Flow in Concentric Annular Ducts," *Heat Transfer Engineering*, vol. 30, pp. 431-436, 2009.

[4] G Lu and J Wang, "Experimental Investigation on Heat Transfer Characteristics of Water Flow in a Narrow Annulus," *Applied Thermal Engineering*, vol. 28, pp. 8-13, 2008.

[5] P.K Swamee, N Aggarwal, and V Aggarwal, "Optimum Design of Double Pipe Heat Exchanger," *International Journal of Heat and Mass Transfer*, vol. 51, pp. 2260-2266, 2008.

[6] A.M Kaneda, B Yu, H Ozoe, and S.W Churchill, "The Characteristics of Turbulent Flow and Convection in Concentric Circular Annuli," *International Journal of Heat and Mass Transfer*, no. 46, pp. 5045-5057, 2003.

[7] O.C Jones and J.C.M Leung, "An Improvement in the Calculation of Turbulent Friction in Smooth Concentric Annuli," *Journal of Fluids Engineering*, vol. 103, pp. 615-623, 1981.

[8] F.W Dittus and L.M.K Boelter, "University of California, Berkeley," *Publications on Engineering*, vol. 2, p. 443, 1930.

[9] C.O Popiel and J Wojtkowiak, "Simple Formulas for Thermophysical Properties of Liquid Water for Heat Transfer Calculations," *Heat Transfer Engineering*, vol. 19, no. 3, pp. 87 - 101, 1998.

[10] YA Cengel, *Heat and Mass Transfer: A Practical Approach*, 3rd ed.: McGraw-Hill, 2006.

[11] S Kline and F McClintock, "Describing Uncertainties in Single-Sample Experiments," *Mechanical Engineering*, vol. 75, pp. 2-8, 1969.

[12] D.E Briggs and E.H Young, "Modified Wilson Plot

Technique for Obtaining Heat Transfer Correlations for Shell and Tube Heat Exchangers," *Chemical Engineering Progress Symposium*, vol. 65, pp. 35-45, 1969.

[13] H.F Khartabil and R.N Christensen, "An Improved Scheme for Determining Heat Transfer Correlations From Heat Exchanger Regression Models with Three Unknowns," *Experimental Thermal and Fluid Science*, vol. 5, pp. 808-819, 1992.

[14] M.P Ntuli, J Dirker, and J.P Meyer, "Heat Transfer and Pressure Drop Coefficients for Turbulent Flow in Concentric Annular Ducts," in *CHISA*, Prague, 2010.